Chemical Solution Deposition of Lead Selenide Films: A Mechanistic and Structural Study

Sasha Gorer,[†] Ana Albu-Yaron,[‡] and Gary Hodes*,[†]

Department of Materials and Interfaces, Weizmann Institute of Science, Rehovot 76100, Israel, and ARO, The Volcani Centre, POB 6, Bet Dagan 50250, Israel

Received January 31, 1995. Revised Manuscript Received April 5, 1995[⊗]

Chemical solution deposition of PbSe films is shown to proceed via two different mechanisms—an ion-by-ion or a cluster mechanism. Here we show how conditions can be chosen where either one or both mechanisms occur, leading to fine control of the film properties. Three different complexing agents for the Pb are discussed, and the unique characteristics of the films obtained using each complexant described and explained. The combination of control of both complexant and deposition mechanism results in films with very different structural properties in terms of crystallite size (3 nm to microns), macrostructure, presence of an amorphous PbSe matrix, and the formation of a novel, rhombohedral form of PbSe. A modified deposition technique, whereby a film of a basic lead carbonate is first chemically deposited and then converted by selenosulfate solution to PbSe, is described.

1. Introduction

Chemical solution deposition (CD) of semiconductor films is a well-established, if somewhat neglected, technique compared with many other methods of thin-film deposition. Our interest in this technique stems from our observation of large quantum size effects—and accompanying large changes in optoelectronic properties—in semiconductor films due to their nanocrystalline structure.[1,2] Since these changes are a direct function of the crystal size, control of crystal size allows control over the optoelectronic properties of films.

While many different semiconductors have been prepared by CD, by far the greatest emphasis has been on Cd and Pb chalcogenides (ref 3, which appears to be the only comprehensive review written on this technique, gives a good background on the earlier literature). PbS and PbSe have been of particular interest due to their use as IR detectors, as first described by Bose.[4] Since they provide relatively good performance and are simple to fabricate as thin films, these detectors are still widely used despite the increasing number of alternatives now available. The two methods used to manufacture these films on a commercial scale are CD and vacuum evaporation.[5]

The mechanism of the CD process has been the subject of much discussion. The basic mechanism, known as the ion-by-ion mechanism, is based on reaction between free metal ions M^{n+} (often Cd or Pb ions) present in low concentration by complexation of a M salt, and slowly generated sulfide or selenide ion ($S(Se)^{2-}$ or, more probable, $HS(Se)^-$, designated here as X^{2-}) typically formed by slow hydrolysis of thiourea (selenourea or selenosulfate). This results in precipitation of MX when the product of the concentrations of M^{n+} and X^{2-} is greater than the solubility product, K_{sp}, of MX. In a second mechanism, the cluster mechanism, film growth occurs by adsorption and coagulation of colloidal particles—either of MX or M–hydroxide—onto the substrate. If the hydroxide is involved, this will react further with X^{2-} to form MX. The presence of M–hydroxide as a reaction intermediate was sometimes obvious from the presence of a visible suspension of the hydroxide in the CD solution.[6] However, it has been shown that even when no visible hydroxide suspension formed in the solution, the hydroxide mechanism might still occur by adsorption of colloidal particles of hydroxide—not visible to the naked eye—on the substrate.[7–9]

For metal selenides, while selenourea or one of its derivatives was originally used as the Se source, selenosulfate ion, prepared by dissolving elemental Se in sulfite solution, was shown to work well as a Se source while being much simpler to prepare and much more stable than the selenourea compounds[10,11] and has essentially replaced the latter as the Se source in CD.

We have recently described the conditions where the mechanism for CD of CdSe changes from a cluster mechanism to an ion-by-ion one, corresponding to the presence or absence respectively of colloidal $Cd(OH)_2$ in the deposition solution and also showed the applicability of these results to other semiconductors, namely, PbSe and CdS.[9] The changeover in mechanism is manifested by a change in the crystallite size of the semiconductor. However, while there are many similarities in the mechanism of CD of CdSe and PbSe, it was clear that

† Weizmann Institute of Science.
‡ The Volcani Centre.
⊗ Abstract published in *Advance ACS Abstracts,* May 15, 1995.

(1) Hodes, G.; Albu-Yaron, A., Decker, F.; Motisuke, P. *Phys. Rev. B* **1987**, *36*, 4215.
(2) Hodes, G.; Albu-Yaron, A. *Proc. Electrochem. Soc.* **1988**, *88–14*, 298.
(3) Chopra, K. L.; Kainthla, R. C.; Pandya, D. K.; Thakoor, A. P. *Phys. Thin Films* **1982**, *12*, 167.
(4) Bose, J. C. U.S. Patent 755,840, 1904.
(5) Johnson, T. H. *Proc. SPIE* **1983**, 60.
(6) Kainthla, R. C.; Pandya, D. K.; Chopra, K. L. *J. Electrochem. Soc.* **1980**, *127*, 277.
(7) Betenkov, N. D.; Medvedev, V. P.; Zhukovskaya, A. S.; Kitaev, G. A. *Radiokhimiya* **1978**, *20*, 608.
(8) Rieke P. C.; Bentjen, S. B. *Chem. Mater.* **1993**, *5*, 43.
(9) Gorer S.; Hodes, G. *J. Phys. Chem.* **1994**, *98*, 5338.
(10) Glistenko, N. I.; Eremina, A. A. *Zh. Neorg. Khim.* **1960**, *5*, 5.
(11) Fofanov G. M.; Kitaev, G. A. *Russ. J. Inorg. Chem.* **1969**, *14*, 322.

0897-4756/95/2807-1243$09.00/0

there were also some fundamental differences, due largely to differences in the chemistry of the hydroxide precursors. The present paper describes specifically the mechanism of the CD process for PbSe and shows how very different films, in terms of the crystallite size and appearance of an amorphous phase, can be obtained. In contrast to many other studies on CD, this paper considers primarily mechanistic and structural factors rather than kinetics ones, since our interest is largely in the size of the crystallites obtained in these films. In addition, since TEM is the basic technique used in this study, it is confined to films which are thin enough to be directly measured by this technique, i.e., no more than 100 nm thick.

2. Experimental Section

Film Deposition. The deposition of the films has been carried out using 3 different complexing agents: trisodium citrate (TSC), potassium nitrilotriacetate (NTA), and potassium hydroxide (KOH).

For the depositions from the TSC bath, the following stock solutions were made up (using deionized water): 0.5 M lead acetate, 1 M TSC, and 0.2 M sodium selenosulfate (Na_2SeSO_3) in excess Na_2SO_3, prepared by stirring 0.2 M Se with 0.5 M Na_2SO_3 at ca. 70 °C for several hours. The deposition solution was prepared by diluting the 0.5 M lead acetate solution with water, then adding the TSC solution, and adjusting the pH with KOH to 10. Finally, Na_2SeSO_3 was added, giving a pH ≤10.8, and then was adjusted to exactly 10.8. The composition of the final solution was 60 mM Pb^{2+}, 50 mM Na_2SeSO_3, and 160−320 mM TSC.

For the depositions from the NTA bath, the same stock solutions were used as above except that 0.7 M K_3NTA was substituted for the TSC. The deposition solution was prepared as for PbSe from TSC complex to give a final composition of 60 mM Pb^{2+}, 50 mM Na_2SeSO_3, and 60−70 mM NTA at a pH of 10.8−11.0.

For the PbSe films from KOH complex, concentrated KOH solutions (1 M or greater) were used as the complex stock solution. The deposition solution was prepared as before to give a final composition of 60 mM Pb^{2+}, 50 mM Na_2SeSO_3, and 0.6−4.3 M KOH at a final pH >13. The lead acetate stock solution was added to the KOH; if the reverse procedure was used (addition of KOH to the Pb solution), a precipitate formed which did not readily dissolve unless a large excess of KOH was added. By adding the Pb solution to KOH, a large excess of KOH was maintained (up to a certain concentration of Pb^{2+}) which prevented precipitation of the hydrated oxide.

Microscope glass slides of ca. 40 × 15 × 1 mm in dimensions were used as substrates. They were cleaned in sulphochromic acid and well rinsed in deionized water prior to the deposition. The substrate was placed at an angle (typically ca. 20° off normal) in the solution, which was then placed in a thermostat at the required temperature and kept in the dark. The film deposited on the lower side of substrate was retained for the various measurements. It was strongly adherent. The deposition time depended on the conditions and the required thickness (20−80 nm for most films). It was typically several hours but could range from tens of minutes to days. Gold substrates were prepared by evaporating 35 nm of Au on glass slides at room temperature and then annealing in air for 3 h at 250 °C.[12] They were immersed in the deposition solution (in most cases, Se-free) for a short time (1−3 min) and then rinsed with water. Films were separated from the glass by immersing them in 1−3% HF.

Optical Spectra of the Deposition Solutions. Optical absorption spectra of the solutions were recorded at room temperature on a two-beam Uvikon 810 spectrophotometer in the 250−600 nm region using 1 cm quartz cuvettes.

(12) Golan, Y.; Margulis, L.; Rubinstein, I. *Surf. Sci.* **1992**, *264*, 312.

Table 1. Stability Constants of the Three Pb Complexes

complex	K_s
TSC [$Pb(citrate)^-$]	6.1
NTA [$Pb(NTA)^-$]	11.3
OH^- [$HPbO_2^-$]	13.9

X-ray Powder Diffraction. Powder X-ray diffraction (XRD) spectra of films deposited on glass or Ti were recorded on a Rigaku RU-200B Rotaflex diffractometer operating in the Bragg configuration using Cu Kα radiation. The accelerating voltage was set at 56 kV with a 170 mA flux. Scatter and diffraction slits of 0.5° and a 0.3 mm collection slit were used.

Transmission Electron Microscopy (TEM). Two sets of specimens were prepared for observation by TEM—plan view specimens of stripped (using dilute HF) films and cross-sectional specimens prepared by microtomy. Conventional medium-resolution TEM images and selected area diffraction (SAD) patterns were obtained using a Philips EM-400T electron microscope operating at 120 kV. High-resolution (HR) TEM in plan view was carried out on a JEOL 4000EX operating at 200 kV. The point-to-point resolution of the microscope was better than 0.18 nm at 200 kV.

Light-scattering experiments were carried out on the various deposition solutions without selenosulfate (designated as Se-free solutions). Shining short-wavelength laser light (488 nm from a Coherent Innova 90 Ar laser) through the solution allowed the presence of an otherwise invisible colloid in the solution to be visualized, due to scattering of the laser beam by the colloidal particles.

The films were chemically analyzed by **X-ray photoelectron spectra (XPS**, Mg Kα photoline), **TEM/EDS**, **EDS/STEM**, **atomic absorption spectroscopy (AAS)**, with a detection limit of 1 ppb and **Rutherford backscattering (RBS)** with the 3-MeV positive ion accelerator of a Van der Graaf generator.

3. Results

Most published work on CD PbSe has been carried out using trisodium citrate (TSC) as the complexing agent. We have used this complex for the major part of our study. We will therefore first describe our results using this complex and later describe results with other complexes with emphasis on differences in the PbSe films obtained using the different complexes. The stability constants of the three Pb complexes are shown in Table 1 for comparison. The hydroxide complex is assumed to be the plumbite ion, $HPbO_2^-$, since Pb^{2+} dissolves in excess alkali metal hydroxide to give this ion and the measured potential of this solution is very close to the literature value for plumbite. The complexing strength increases in the order TSC < NTA < OH^-.

3.1. Deposition from TSC Complex. 3.1.a. Nucleation of Lead Hydroxide. Since, as we noted previously, the deposition mechanism was dependent on whether or not a colloidal hydroxide was present in the deposition solution, the conditions for the occurrence and the nature of such a colloidal species is clearly of importance. This colloidal species depends on the free metal ion concentration and, among other factors, this concentration is a function of the complex-to-metal ratio (TSC:Pb in the present case). For the Pb−TSC system, a colloidal hydroxide species was always found to exist; however, the concentration of this species and also the dominant deposition mechanism (and hence crystallite size) were primarily dependent on the TSC:Pb ratio. Here we use the terms LC (low complex-to-metal cation ratio; predominantly cluster deposition mechanism) and HC (high complex-to-metal cation ratio; ion-by-ion deposition mechanism) to define the two different types

of deposition solutions. We will first relate the relative concentrations of the colloidal lead hydroxide in the Se-free deposition solutions to the solution compositions and describe nucleation of this solid phase on thin gold films on glass.

Lead hydroxide has been reported to absorb in the UV with an onset of 345 nm.[13] No simple $Pb(OH)_2$ species is known to exist, and this "hydroxide" is probably a hydrated oxide. We find that the selenosulfate-free (which we will refer to as Se-free) deposition solution absorbs in the same spectral region which we can correlate with our solid phase. XRD of this phase—measured from powders collected by passing large quantities (ca. 500 mL) of Se-free deposition solutions through fine filter paper—shows very broad peaks which can be correlated either with the composition $3PbO_xH_2O$, (powder file 22−1134) or $6PbO_x0{\cdot}3H_2O$ (powder file 21-474); we will refer to this material as Pb−OH for convenience. From the peak widths and assuming size broadening, a crystal size of <10 nm can be estimated (it may be considerably smaller than this, but because of the relatively large number of reflections involved, a smaller size would not be resolved). A small percentage (up to ca. 5%) of a phase corresponding to the composition $6PbCO_3{\cdot}3Pb(OH)_2{\cdot}PbO$ (which for simplicity, we will refer to in this paper as Pb−OH−C) and made up of much larger crystals (ca. 100 nm) is also sometimes found. This phase is absent in degassed solutions or in solutions made up from freshly deionized or distilled water.

Figure 1 shows the dependence of the UV absorption of Se-free deposition solutions on TSC:Pb ratio (a), pH (b), and time (c). Note that the reference solution is different in the three cases. The steep increase in absorption at ca. 310 nm is due to components of the solutions other than Pb−OH and does not interest us here; rather it is the onset of absorption due to colloidal Pb−OH which is of importance. Figure 1a shows that there is a gradual increase in the Pb−OH absorption with decrease in TSC:Pb ratio. Figure 1b shows the corresponding gradual increase in Pb−OH absorption with increase in pH. This is for a fairly low (LC) TSC:Pb ratio; for a high ratio (HC) deposition, where TSC:Pb = 4, for example, there is only a small change in the absorption over this pH range. Another factor which affects this absorption is aging of the solution. Figure 1c shows the absorption of a LC solution as a function of time. The Pb−OH absorption increases strongly with time, and after 90 min, visible Pb-OH formation can be seen in the solution as seen by the increase in optical density at longer wavelengths due to scattering by aggregated clusters. This aging is accompanied by a modest increase in pH (shown in Figure 1c). A somewhat larger pH increase—ca. 0.5 pH unit—occurs for a normal deposition solution (containing Se).

Laser scattering, using a blue laser, was employed in our previous study to find the conditions where $Cd(OH)_2$ just began to occur as a solid phase in CdSe deposition solutions.[9] In the case of the PbSe/TSC system, this method was not suitable as Pb−OH was always present, with a smooth change in concentration with change in solution composition. Here the presence

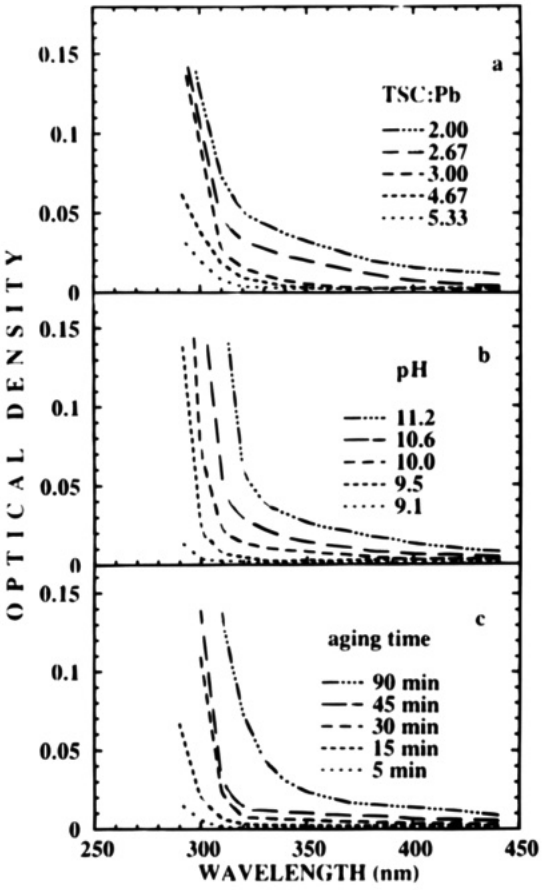

Figure 1. Dependence of the UV absorption spectra of aqueous solutions of lead acetate and TSC on TSC:Pb ratio (a), pH (b), and time (c). The reference solutions were TSC:Pb = 6 (a), pH = 8.5 (b), and fresh solution for each measurement (c).

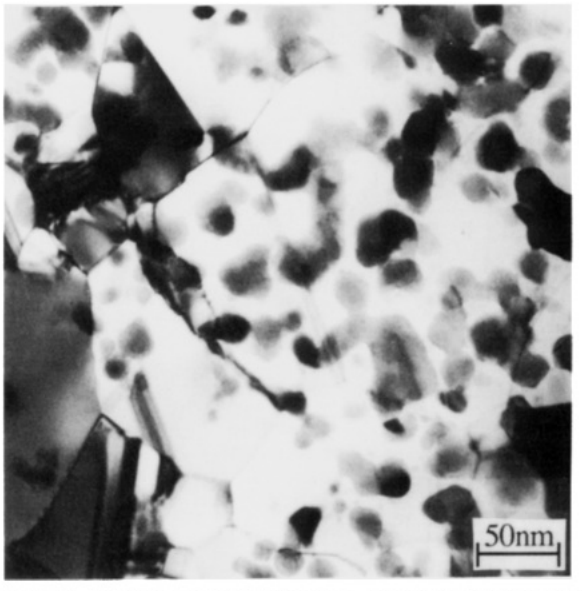

Figure 2. TEM image of a thin-film Au substrate immersed in a Se-free TSC deposition solution (LC) for 3 min.

of Pb−OH clusters in solution was correlated with nucleation on a thin Au film (30 nm) on a glass substrate. Figure 2 shows a TEM image of such a Au substrate after three minutes immersion in a Se-free deposition solution. From the ED pattern (not shown), the grains can be assigned to Pb−OH. Immersion for only 1 min resulted in no visible deposition; i.e., the initial nucleation required some minutes to occur. The

(13) Berton, A. *Compt. Rend.* **1938**, *207*, 625.

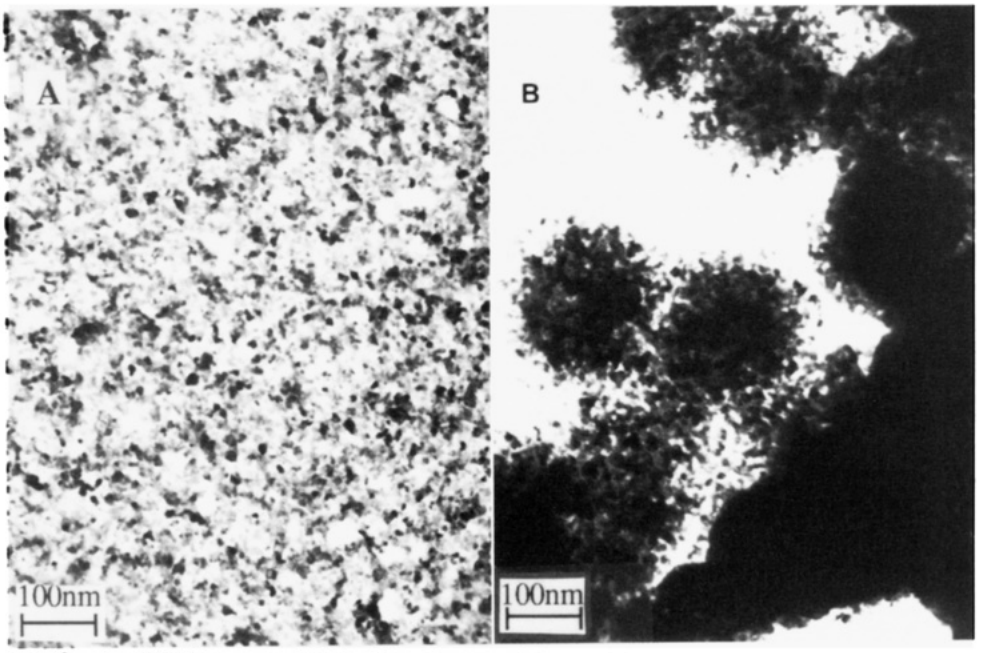

Figure 3. Low-magnification TEM images of PbSe films deposited from TSC solution at 0 °C on glass substrates under LC (A) and HC (B) deposition conditions.

Table 2. Crystal Sizes, Measured by TEM and XRD, of Various Films Deposited from the Three Complexants under Different Condition[a]

complex	preparation conditions (complex:Pb ratio, temp, thickness)	size from TEM (nm)	size from XRD (nm)
TSC	2.67 (LC), 0 °C, 20 nm	3.5–4.0	- - -
	2.67 (LC), 0 °C, 60 nm	3.5–4.0, 6.0–12.0	6.5
	2.67 (LC), 60 °C, 20 nm	4.0–4.5	- - -
	2.67 (LC), 60 °C, 60 nm	4.0–4.5, 6.0–12.0	7.2
	5.33 (HC), 0 °C, 70–80 nm	8.0–15.0	10.0
	5.33 (HC), 60 °C, 70–80 nm	8.0–15.0	15.0
NTA	1.00 (LC), 0 °C, 30 nm	3.5–7.0	
	1.00 (LC), 0 °C, 70 nm	3.5–7.0, 9.0–25.0	10.0
	1.00 (LC), 20 °C, 70 nm		13.0
	1.00 (LC), 40 °C, 70 nm		17.5
	1.00 (LC), 60 °C, 30 nm	5.5–7.0	- - -
	1.00 (LC), 60 °C, 70 nm	5.5–7.0, 15.0–35.0	30.0
	1.17 (HC), 0 °C, 70–80 nm	10–30	20.0
	1.17 (HC), 60 °C, 70–80 nm	15–35	30.0
KOH	10.0 (LC), 0 °C, 70–80 nm	3.5–4.0	<5.0
	72.0 (HC), 0 °C, 80–100 nm	3.5–4.0, 300–500	30.0
	10.0 (LC), 30 °C, 70–80 nm	3.5–4.0	<5.0
	36.0 (HC), 30 °C, 100 nm	1000–2000	
	5.0 (LC), 60 °C, 70–80 nm	10.0–20.0	12.0
	36.0 (HC), 60 °C, 80–100 nm	1000 (SEM)	
	72.0 (HC), 80 °C, 100–200 nm	ca. 2000 (SEM) hexagonal	

[a] The larger crystal sizes (> ca. 50 nm) could not be measured by XRD due to instrument broadening. Broken lines represent XRD data which showed no peaks.

same experiment carried out in a Se-containing deposition solution showed the presence of PbSe nucleii after 3 min.

3.1.b. PbSe Films—TEM. There is a clear visible difference between the PbSe films produced in the LC and HC types of deposition solution, particularly for thin films. While the former are reasonably homogeneous and specularly reflecting, even for thin films, the latter have a more gray appearance (although still adherent to the substrate) and appear very patchy with considerable light scattering as thin films (in contrast to the very low scattering characteristic of the LC films). The low-magnification TEM micrographs in Figure 3 clearly show that the HC films are made up of aggregates of individual crystallites (Figure 3B) compared with the more homogeneous (on the same size scale) nature of the LC films (3A). Thicker HC films become more reflecting and metallic in appearance with visibly better transmission in the subbandgap region, the latter occurring since scattering decreases more than the specular reflectance increases.

Typical images of LC and HC films at higher magnification are shown in Figure 4A–C, respectively. The exact sizes of the crystallites in the films depends on other factors as well, in particular on film thickness and on deposition temperature. The range of sizes for different films is given in Table 2. The LC films (except for very thin films—ca. 20 nm—which contain only small crystals) are made up of micron-sized domains of either small crystallites (Figure 4A) or large crystallites with a defined angular appearance (Figure 4B); the proportion between the two domains depends on the film thickness, but for the films studied here (usually not thicker than 100 nm), only a relatively small proportion

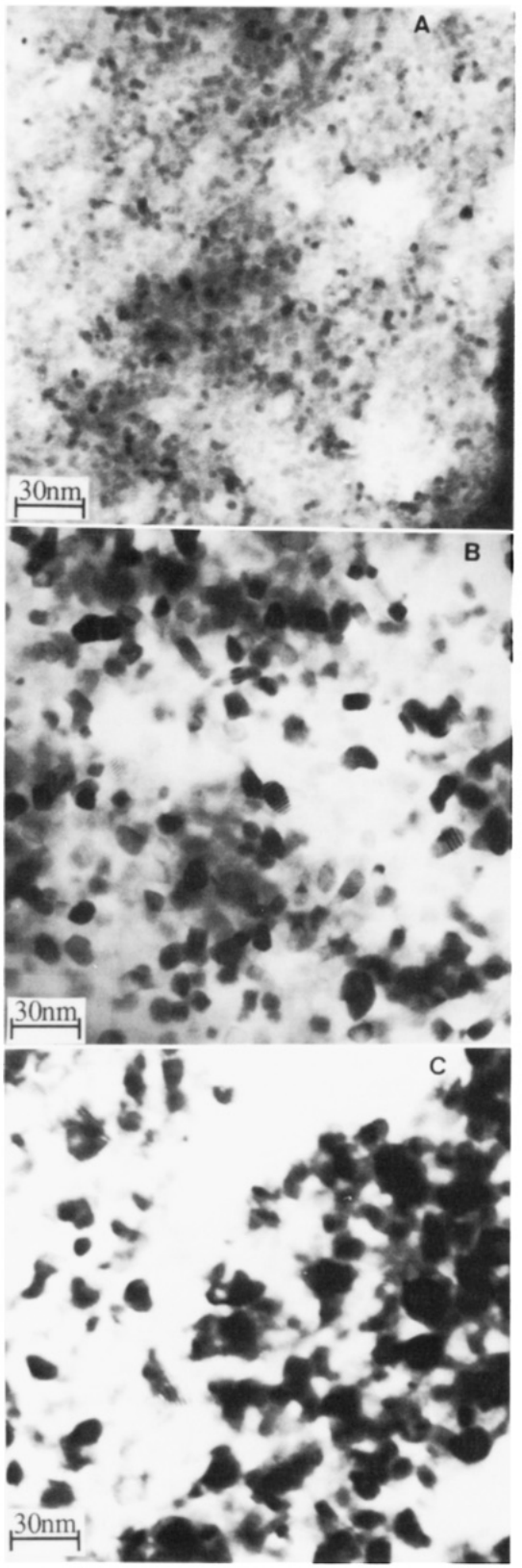

Figure 4. TEM images of PbSe films deposited from TSC solution at 0 °C on glass substrates under LC (A, B) and HC (C) deposition conditions.

of the film (typically <10%) is made up of the large-crystallite domains. The size distribution of the crystallites can be seen to be rather broad. The crystallite sizes are typically 4 nm for the small ones, 6−12 nm for the larger crystallites in the LC films, and 8−15 nm for those in the HC films. Analysis of various SAD patterns of the films showed them to be composed of

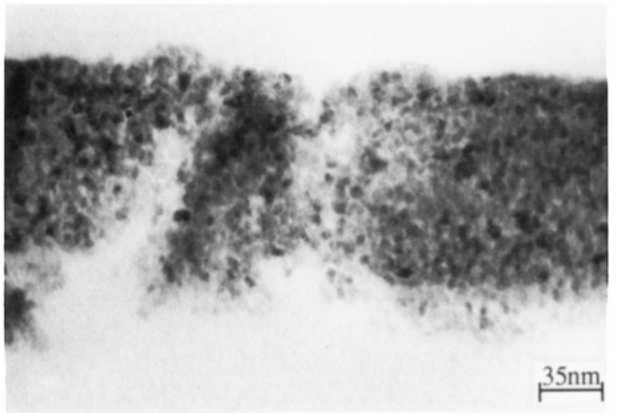

Figure 5. Cross-sectional TEM image of a "thick" (ca. 130 nm) PbSe film deposited from TSC solution under LC conditions at 4 °C.

cubic PbSe with lattice parameters identical to literature values, even for the smallest crystallites.

That the crystallite size is fairly constant throughout the thickness of the small crystal domains, which make up most of the film, is seen from a cross-sectional TEM image of a "thick" (ca. 130 nm) LC film (Figure 5). This micrograph clearly reveals that the film is made up of very small spherical grains ca. 3−4 nm in diameter, held in an apparently amorphous matrix and uniformly distributed throughout the thickness of the film. The films are cohesive as they were not affected by microtomy.

Thicker films without the large crystallite domains can be made if the selenosulfate concentration is lowered considerably (ca. 15 mM instead of the more usually used 50 mM). In this case, films of >70 nm thick can be made which are constituted entirely from small crystals like those shown in Figure 4A.

Of particular interest is the presence of an apparently amorphous matrix surrounding individual crystallites. This matrix appears to form mainly in the early stages of the growth of the *LC* films. The TEM micrographs in Figure 6 illustrate two nearby areas typical of such an *LC* film in the early stages of deposition. The TEM image in Figure 6A shows that the film consists of small crystallites (the dark round particles) of ca. 5 nm in diameter, uniformly distributed within a continuous (amorphous) matrix. The image in Figure 6C shows predominantly this (amorphous) matrix. The corresponding selected area diffraction (SAD) patterns (Figure 6B,D, respectively) clearly support the assignment of the films in these areas: while Figure 6B displays fairly sharp and continuous diffraction rings (all fitting most of the reflections of cubic PbSe) superimposed on two broad diffuse rings which correspond to mainly the (220) and (311) reflections of PbSe, Figure 6D shows the presence of only these broad and diffuse rings. We associate the sharp and continuous ring pattern in Figure 6B with many randomly oriented, small crystallites of cubic PbSe shown in the respective TEM image, and the broad rings in Figure 6B,D with the matrix itself. The similarity of the sharp and diffuse diffraction patterns is consistent with the assignment of a composition of PbSe to the amorphous matrix. Figure 6E shows the corresponding HRTEM image of the film shown in Figure 6A. Most of the particles are 4−5 nm in diameter and exhibit different crystallographic orientations. They appear not to cluster

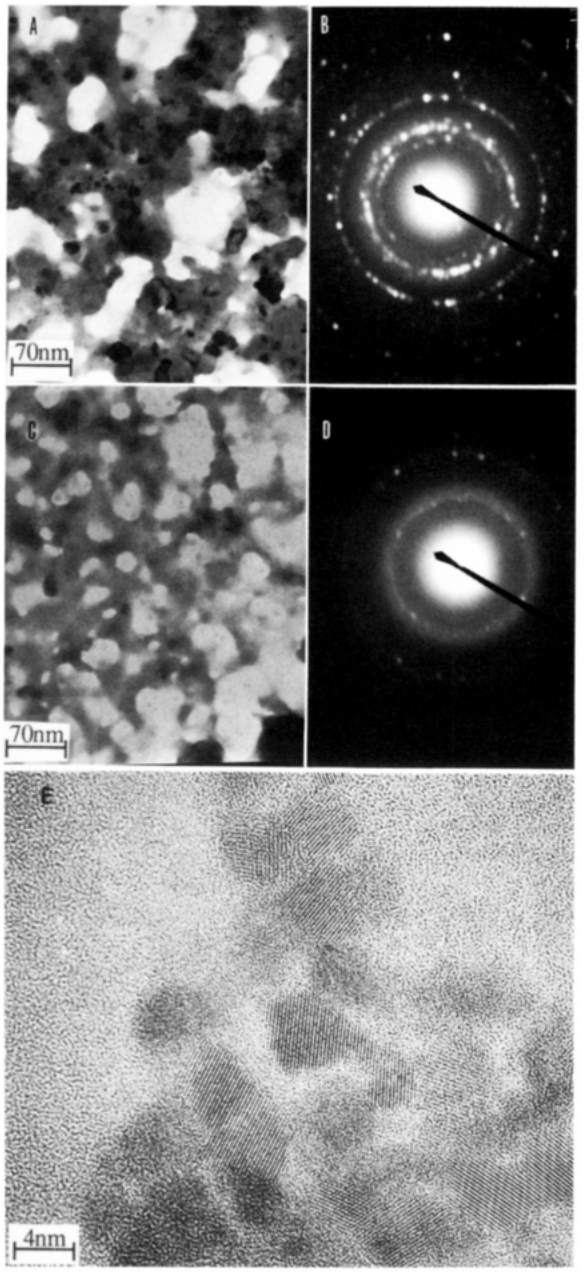

Figure 6. TEM micrographs (plan view) of a PbSe LC-deposited (5 °C) specimen. (A) A typical area showing that the film contains small crystallites embedded in an amorphous matrix; (B) SAD pattern corresponding to (A); (C) a nearby area showing mainly the amorphous matrix; (D) SAD pattern corresponding to (C); (E) high-resolution image of the film shown in (A).

together in any preferential manner, and they are nearly perfect and free from lattice defects. The HR-TEM confirms that films consist of small crystallites of PbSe surrounded by a matrix exhibiting a granular contrast typical of an amorphous material.

3.1.c. X-ray Powder Diffraction (XRD). XRD patterns could only be obtained from films thicker than ca. 30–40 nm. The very thin films described above (20 nm) showed no XRD pattern, even when run under conditions (mainly very slow scan rate) where even thinner films of CdSe showed a very clear signal.

The crystal sizes for various PbSe films, calculated from the widths of the XRD peaks, are given in Table 2. Two typical XRD patterns are shown in Figure 7 of a LC film (7a) and a HC film (7b). The spectrum of the

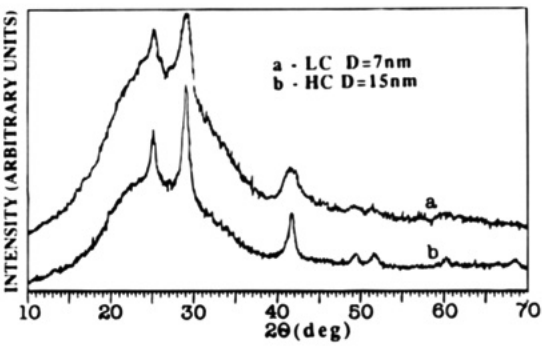

Figure 7. Two typical XRD spectra of PbSe films deposited at 60 °C with different TSC:Pb ratios. The crystal sizes, D, calculated by the Debye–Scherrer formula are shown.

Table 3. Se:Pb and O:Pb Ratios Measured by XPS before and after Sputter Etching (ca. 15 nm Depth)

	$>R_c$		$<R_c$	
composition	as dep	etch	as dep	etch
Pb	1	1	1	1
Se	0.98	0.78	0.6	0.54
O	0.6	0.38	1.7	0.65

LC film appears to show relatively sharp peaks on a background of broader peaks (these broader peaks should not be confused with the very broad glass background from $2\theta = 15–38°$). This makes interpretation difficult. However it is clear from comparison of the TEM and XRD data that the sharper peaks in Figure 7a correspond to the large crystallite domains as in Figure 4b. The crystal sizes of the two types of films are in essential agreement with the TEM results in Figure 4. In addition to PbSe, a small amount (up to 5%) of basic lead carbonate ($Pb_3(CO_3)_2(OH)_2$ powder file 13-131) is sometimes seen as a sharp peak in thicker films (not seen in the examples of Figure 7). This basic carbonate is not found in very thin films, and its appearance is a function of the duration of deposition; its concentration in the films increases with deposition time. Since the deposition solution is normally exposed to air, it is assumed that this basic carbonate forms by reaction of the solution with CO_2 from the air after the selenosulfate has been depleted. Since the XRD peak of this material is sharp, it clearly exists as much larger crystals than those of PbSe.

3.1.d. Chemical Analysis. We have carried out extensive chemical and related physical analyses of these films, mainly to determine the chemical nature of the matrix but also to find out if other constituents were formed in the films and to complement the data obtained from the XRD and TEM measurements. XPS was used to provide an estimate of the composition of the different films. The results for a HC and a LC film are shown in Table 3. The Se:Pb ratio decreases and the O:Pb ratio increases as the crystallite size decreases for both as-deposited and sputter-etched films. The decrease in Se after etch could be due either to a relative surface enrichment of Se or to preferential sputtering of Se compared to Pb. The surface Se for the LC film exhibits two peaks (not shown here)—a selenide peak and a higher binding energy one characteristic of a selenium oxide—the latter of which is removed after sputtering and which is absent in the HC film. RBS was used only qualitatively as the results were difficult to interpret. However, as for XPS, the Pb:Se ratio was found to be >1, with a greater Pb excess at the

Table 4. Values of the Critical Ratio, R_c, for NTA:Pb Solutions Measured by Laser Scattering at Different Temperatures

T (°C)	R_c
0	$1.00 < R < 1.05$
30	$1.08 < R < 1.17$
60	$1.15 < R < 1.25$

beginning of the deposition for the LC films. RBS also indicated the presence of small amounts of S in the films, particularly in the LC ones. AAS was in essential agreement with the above results. However, this method was not reliable, giving high Pb:Se ratios, probably due to loss of Se as H_2Se upon sample preparation by acidic dissolution of the PbSe. TEM/EDS microanalyses were carried out on thin *LC* films containing a large component of the amorphous matrix. While the results were qualitative, due to the difficulty in standardizing the analysis for such thin films, it is notable that no difference was found in the Pb:Se ratio for regions which were predominantly matrix and those which were predominantly crystalline PbSe (as confirmed by ED).

3.2. Deposition from NTA Complex. For films prepared using NTA as complexing agent, a clear separation of the LC and HC conditions for the deposition was observed. Laser scattering experiments of the deposition solutions showed a sharp transition between a cluster-containing and cluster-free solution, as was the case for CdSe[9] and the complex:metal concentration ratio corresponding to this transition has been denoted, in ref 9, by the term "critical ratio" or R_c. The range of compositions where the solution is clear to the eye but shows laser scattering is very narrow. Thus LC films are formed from a solution which is turbid. Table 4 shows the limits of this transition measured at different temperatures. It is clear from the values of NTA:Pb critical ratio (close to unity) that NTA forms a strong 1:1 complex with lead. For this reason also, no deposition at all occurs if the NTA:Pb ratio is much greater than unity; e.g., to obtain HC films at 30 °C, this ratio is limited to a range between ca. 1.08 and 1.17, the exact values depending on the pH as well as temperature. It is therefore not surprising that the formation of *HC* films from the NTA bath is considerably less reproducible than using the other complexing agents.

The visual appearance of both the LC and HC NTA films does not differ much from that of the corresponding TSC films; there is a tendency for the HC NTA films to scatter light to a lesser extent than the HC TSC ones, but both scatter strongly as thin films and become more transparent as their thickness increases. This apparent anomaly is explained in the Discussion. Figure 8 shows low-magnification TEM images of LC (8A) and HC (8B) films. The former are very similar to the LC films from the TSC bath (compare with Figure 3A) while the latter are made up of somewhat larger crystallites than the corresponding TSC films and do not aggregate into tight spherical clumps (compare with Figure 3B).

High-magnification TEM analysis of these films showed a qualitative similarity to those deposited from TSC solutions. For LC films, very thin layers (ca. 20 nm) contain relatively small crystallites while thicker layers are made up of domains of smaller and larger ones. The HC films contain only large crystallites. As with the TSC films, the small crystallite domains make up most of the film (usually >90%). Figure 9 shows

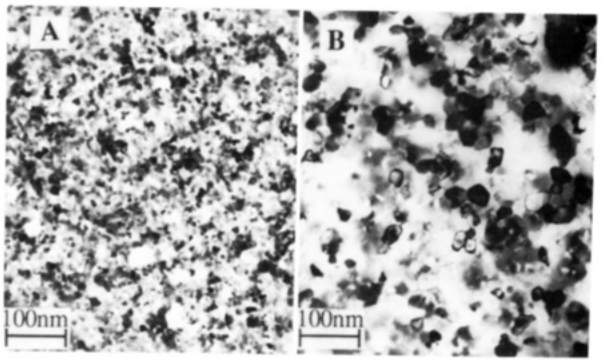

Figure 8. Low-magnification TEM images of PbSe films deposited from NTA solutions at 60 °C on glass under LC (A) and HC (B) conditions.

typical TEM images of three different films—two LC films grown at 0 °C (9A,B) and 60 °C (9C) [the small crystallite domains in these films are similar] and a HC film grown at 60 °C (9D). As for the TSC films, very thin LC films contain only small crystallites, similar in size to those in the small crystallite domains of the thicker films. There is a moderate scatter in the dimensions of the small crystals—typically ranging from 3.5 to 7 nm (9A). The size and size distribution are not strongly temperature dependent. For the large crystal domains, there is a larger scatter in size, and in this case, there is a considerable increase in size with increasing temperature, with most of the crystals in the 9–25 nm range for the 0 °C deposition (9B) and 15–35 nm range (even larger grains are formed, but they appear to be made up of smaller, possibly multiply twinned, crystals) for the 60 °C deposition (9C). The majority of the crystals in the HC films were 15–35 nm in size (9D). Furthermore the macroscopic form of these crystals was different from the large crystal domains of the LC films, with more clustering of the individual crystals into tight aggregates as shown in the low magnification TEM images in Figure 8.

XRD patterns showing the (220) peak of six different PbSe films, with crystallite sizes calculated from the peak widths, are shown in Figure 10. (As for Pb:TSC films, no signal was found for very thin films). For LC films (1–3, 5), the crystallite size grows with increasing temperature, particularly at higher temperatures. For HC films (4, 6), large crystallite sizes are obtained with little temperature dependence. No peak corresponding to basic lead carbonate has been found in these films.

Deposition from Hydroxide Complex. Deposition of PbSe was carried out from solutions containing a KOH:Pb ratio of 5–10, depending on deposition temperature (LC, turbid solution, pH ca. 13.4) and 36–72 (HC, clear to the blue laser, pH ca. 14). As for the NTA complex, there was only a narrow ratio range where the solution was not turbid yet showed laser scattering. In addition, this narrow range was unstable in that the scattering decreased and disappeared with time, i.e., the Pb–OH colloidal phase gradually dissolved, switching over to HC conditions. For this reason, we used relatively low and very high ratios for the LC and HC depositions, respectively, to be sure that these conditions remained valid throughout the deposition.

TEM images of films deposited at 0 and 60 °C are shown in Figure 11. The two-domain structure of the TSC and NTA films was absent here; only small crystallites—mostly in the 3–7 nm range—were ob-

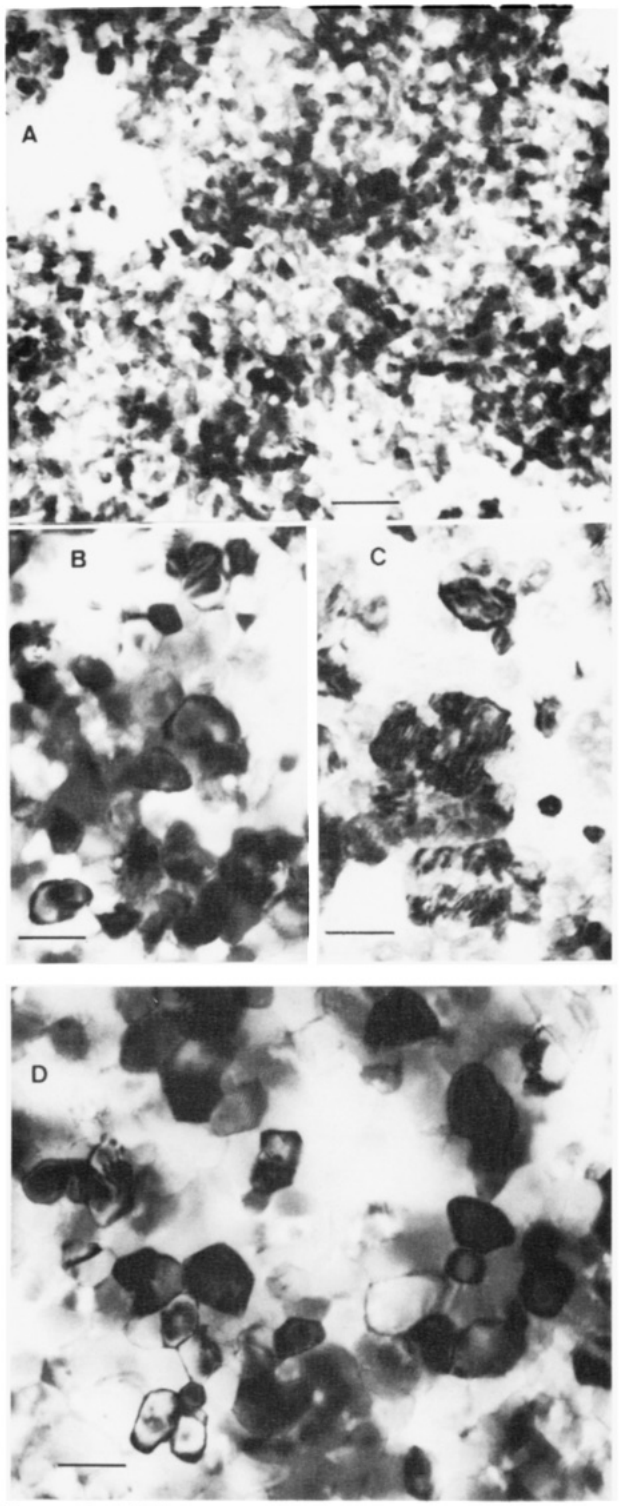

Figure 9. TEM images of PbSe films deposited from NTA solution on glass at 0 °C under LC conditions (A, B); 60 °C, LC conditions (C) and 60 °C, HC conditions (D). Scale bar = 30 nm.

served in low-temperature deposited LC films (11A), even in relatively thick ones, although the size of these crystallites did grow with increasing time in the deposition solution. The crystallites in these films were homogeneously distributed in the film, with occasional small voids probably due to the thickness—ca. 100 nm—of the film (11B). The 0 °C HC films exhibited fairly large, well-defined square-shaped crystals of ca. 300–500 nm cross section covered with approximately spherical (actually slightly polyhedral) aggregates, ca.

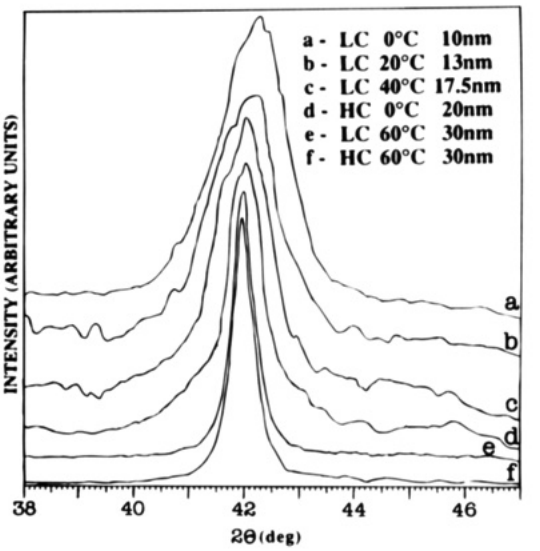

Figure 10. XRD spectra of PbSe films deposited under different conditions from NTA solutions. The calculated crystal sizes, D, are shown.

250 nm in size, of small (ca. 5 nm) crystallites (lower magnification image in Figure 11C). The 60 °C films were rather different; The LC films were made up of crystallites ca. 10–20 nm in size (11D), while the HC films contained only large, square-shaped crystals of ca. 1 μm (11E). The LC films were homogeneous, very transparent (in the nonabsorbing wavelength range—typically >800 nm) and specularly reflecting. The HC films were gray and scattered light strongly.

XRD spectra of some of these films are shown in Figure 12. As for the other small-crystal films, no signal was found for the films containing only very small crystals (0 °C LC; Figure 12a). For the 60 °C HC films, the XRD gave the instrumental line-broadening spectrum, and therefore the only size information obtainable is that the crystals are larger than 50 nm. The 60 °C LC film gave an estimated crystal size of 12 nm, within the range measured directly by TEM. The 0 °C HC film gave a value of 40 nm, very different from the TEM results from the same film (a mixture of 5 and 500 nm crystals). In such a case of two very different crystal sizes, the larger ones are expected to dominate the spectrum.

An anomalous structure forms at high temperatures (80 °C), particularly for thick films which have been left in the deposition solution for long periods of time. Figure 13 shows a scanning electron microscope image of such a film. Large (1–3 μm) hexagonally shaped crystals are observed which microprobe analysis showed to be identical in composition to normal PbSe. XRD of this film (Figure 14) shows two peaks at low angles (2θ = 11.2° and 22.5°) as well as other peaks characteristic of normal cubic PbSe (we do not know whether these latter peaks originate from the hexagonal crystals or from cubic PbSe which is formed in parallel).

The crystal sizes of various films deposited from the three complexants are summarized in Table 2 for ease of comparison.

Selenization of Pb–OH and Pb–OH–C by Selenosulfate. We found that films of Pb–OH–C were slowly deposited, over a period of several days, from a selenosulfate-free, LC deposition solution. The carbonate comes from dissolved atmospheric CO_2; these films

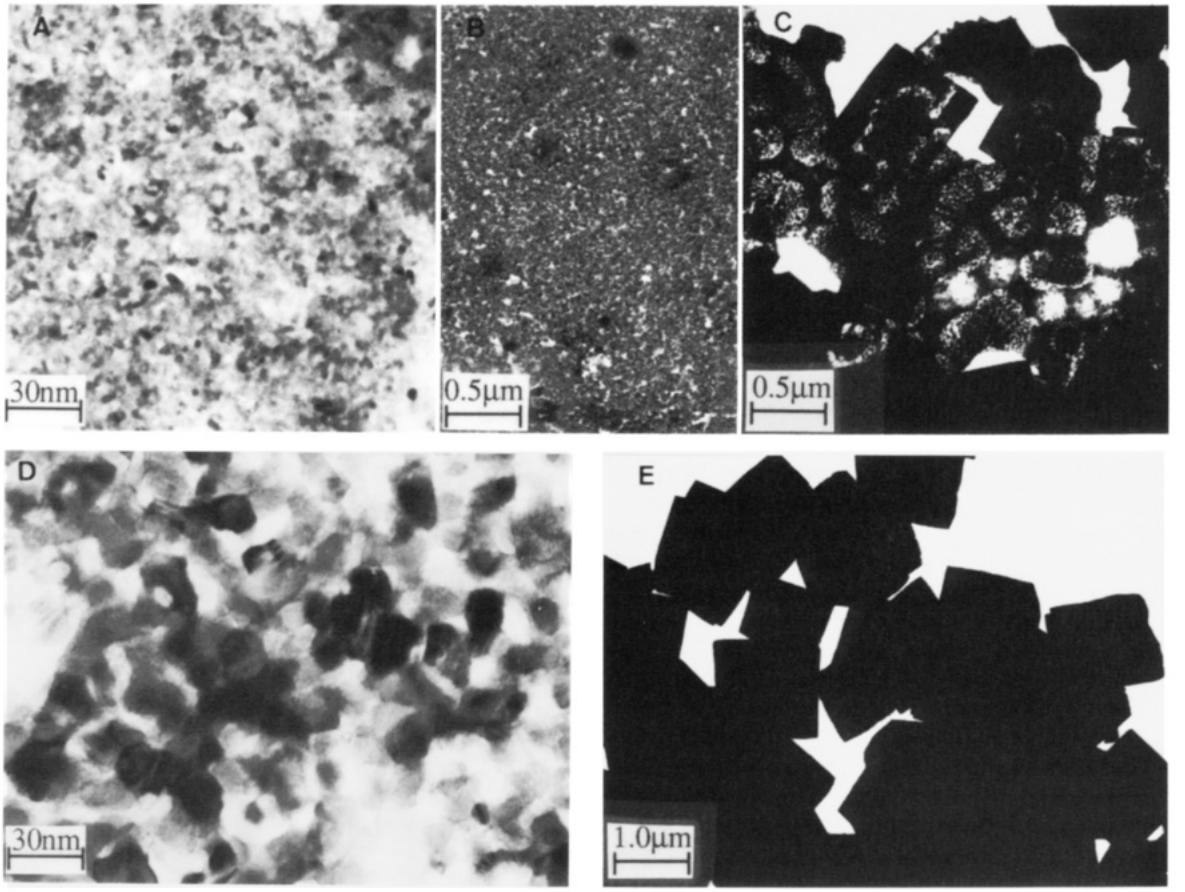

Figure 11. TEM images of PbSe deposited from KOH solution at 0 °C, LC, high magnification (A) and low magnification (B); 0 °C, HC (C), 60 °C, LC (D); 60 °C, HC (E).

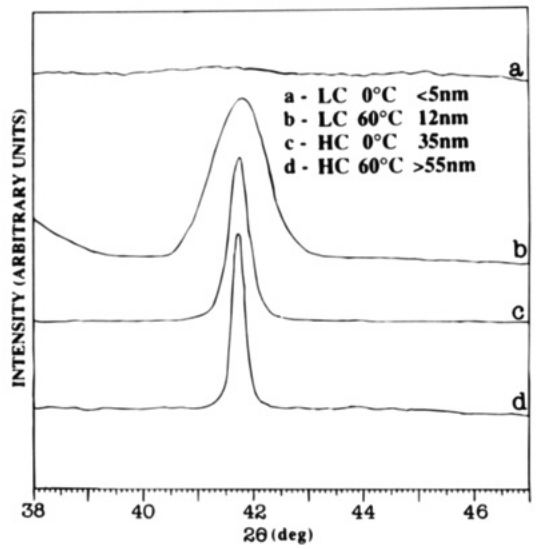

Figure 12. XRD spectra of PbSe films deposited from KOH solution under different conditions. The calculated crystal sizes, *D*, are shown.

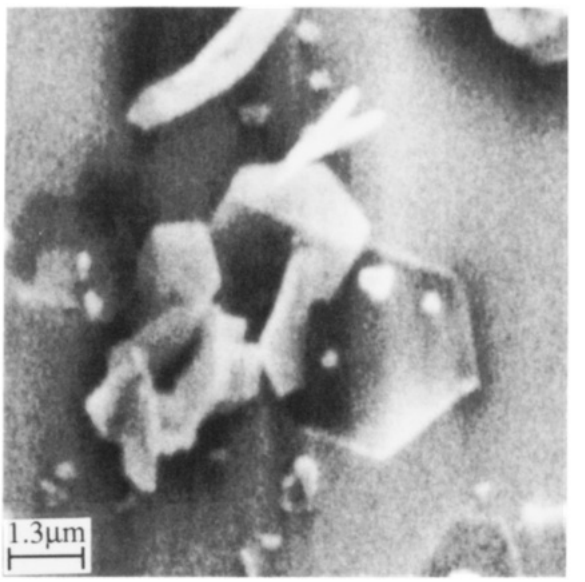

Figure 13. SEM image of hexagonally shaped PbSe crystals deposited from HC KOH solution at 80 °C.

do not form from degassed and well-closed solutions. Immersion of these films in selenosulfate solution resulted in formation of PbSe films. We studied the reaction between these films of Pb−OH−C and selenosulfate solution as a novel method of forming PbSe films and to better understand the mechanism of PbSe deposition.

Figure 15 shows the XRD pattern of a Pb−OH−C film (bottom spectrum) and its change with time after immersing it in a selenosulfate solution. The film transforms almost completely to PbSe. The corresponding TEM and SAD data are shown in Figure 16. The large Pb−OH−C crystals (16A,B) are initially broken down into small PbSe crystals and an amorphous material (16C). Eventually all the Pb−OH−C is converted into large crystals of ca. 200 nm (16D,E,F) which are covered with much smaller PbSe crystals of ca. 15−20 nm (16G) and also some amorphous material seen from the diffuse ring in the ED of 16H. We note that nonbasic lead carbonate ($Pb(CO)_3$) does not react with

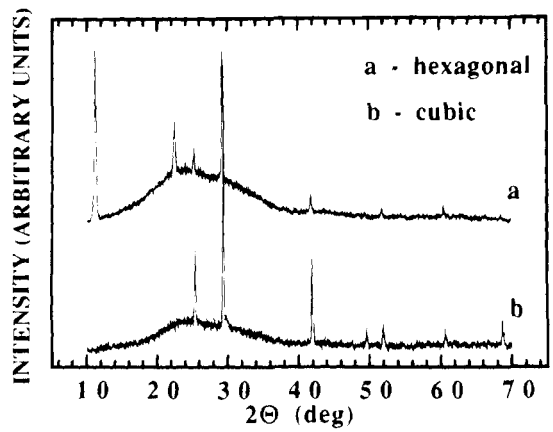

Figure 14. XRD spectra of hexagonally-shaped (a) and cubic (b) PbSe films deposited from HC KOH solution at 80 and 60 °C, respectively.

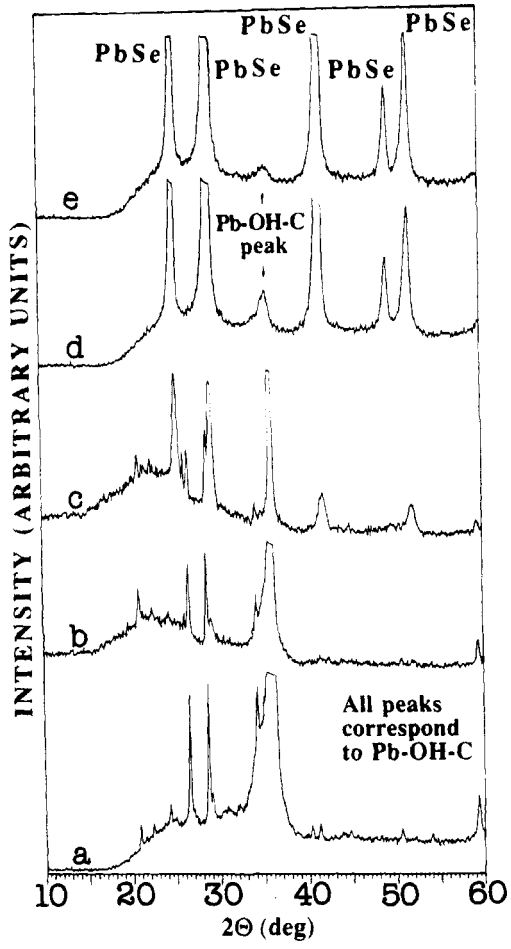

Figure 15. XRD spectra following the process of PbSe formation from the reaction of $6PbCO_3{\cdot}3Pb(OH)_2{\cdot}PbO$ (Pb–OH–C) and Na_2SeSO_3. Pb–OH–C before reaction (a); after 1.5 min reaction (b); after 3 min (c); after 4.5 min (d); after 6 min (e).

selenosulfate. Lead oxide hydrate ("lead hydroxide")—obtained by mixing lead(II) acetate and KOH, and which is assumed to be the intermediate species in all the LC depositions—does, on the other hand, react with selenosulfate. We have not been able to deposit films (other than very sparse deposits as shown in Figure 2) of Pb–OH, and for this reason, we have carried out the parallel reaction with precipitated powders of this compound. Figure 17 shows the change in the XRD pattern of this precipitate during reaction with selenosulfate. As with the Pb–OH–C reaction, this reaction also passes through an intermediate amorphous phase. EDS/STEM measurements of the material corresponding to the intermediate stage of the reaction confirm that the amorphous material is PbSe.

Discussion

We will discuss first the TSC:Pb results, then the other complexing systems will be treated in the framework of the results obtained from the TSC system. To begin with, it is worth recalling the preliminary information we already published concerning the mechanism of PbSe CD and the differences between the PbSe and CdSe deposition.[9]

For CdSe, the mechanism proceeds either via selenization of $Cd(OH)_2$ which is present in the deposition solution as a colloidal species (LC deposition, the cluster mechanism, where CdSe was deposited in the bulk of the solution as well as on the substrate) or, where no solid hydroxide species is present in the solution, by an ion-by-ion mechanism (HC deposition, CdSe deposition on substrate only) which depends on generation of sufficient free Cd^{2+} and HSe^- to exceed the solubility product, K_{sp}, of CdSe. The two different mechanisms resulted in different crystallite sizes in the films.

For PbSe deposition from the TSC bath, the difference between the two mechanisms was not as clear cut as for CdSe. A colloidal Pb–OH species was always found to be present in the bath but in amounts which varied widely depending on the deposition conditions. As with CdSe, smaller or larger crystallite films could be grown depending on the complex:Pb ratio (among other factors), but the difference in size of the crystallites was, in general, less than obtained with CdSe. We suggested that larger crystallites of PbSe could be obtained from solutions containing some solid Pb–OH species (in contrast to CdSe where large crystallites were only obtained if no solid hydroxide was present) because of the lower K_{sp} of PbSe compared with CdSe, allowing the ion-by-ion process to proceed at lower concentrations of the constituent ions. Since the ion-by-ion deposition depends on the product of the concentrations of both lead and selenium species, decreasing the concentration of selenium will favor the cluster deposition (which should not be strongly dependent on the Se concentration) over the ion-by-ion mechanism (which is more strongly affected by this parameter). This explains why lowering the selenium concentration prevents formation of the large crystallite domains.

The relative concentrations of Pb–OH in Se-free deposition solutions, shown in Figure 1, give the conditions where a preferential cluster or ion-by-ion mechanism is assumed to occur. As expected, the concentration of this solid phase is very dependent on both TSC:Pb ratio (as shown also in ref 9) and on pH. Less expected is the gradual increase in the solid phase concentration as a function of time (Figure 1c), which parallels a gradual increase in pH. This increase in pH, which does not occur in a closed, degassed solution, could result from reaction between the Pb–OH and (bi)carbonate formed from dissolved CO_2 to give Pb–OH–C which is found in films deposited over a relatively long period of time. Such a reaction would produce OH^- ions—i.e., an increase in pH. The increase in pH will cause increased formation of the solid phase as observed

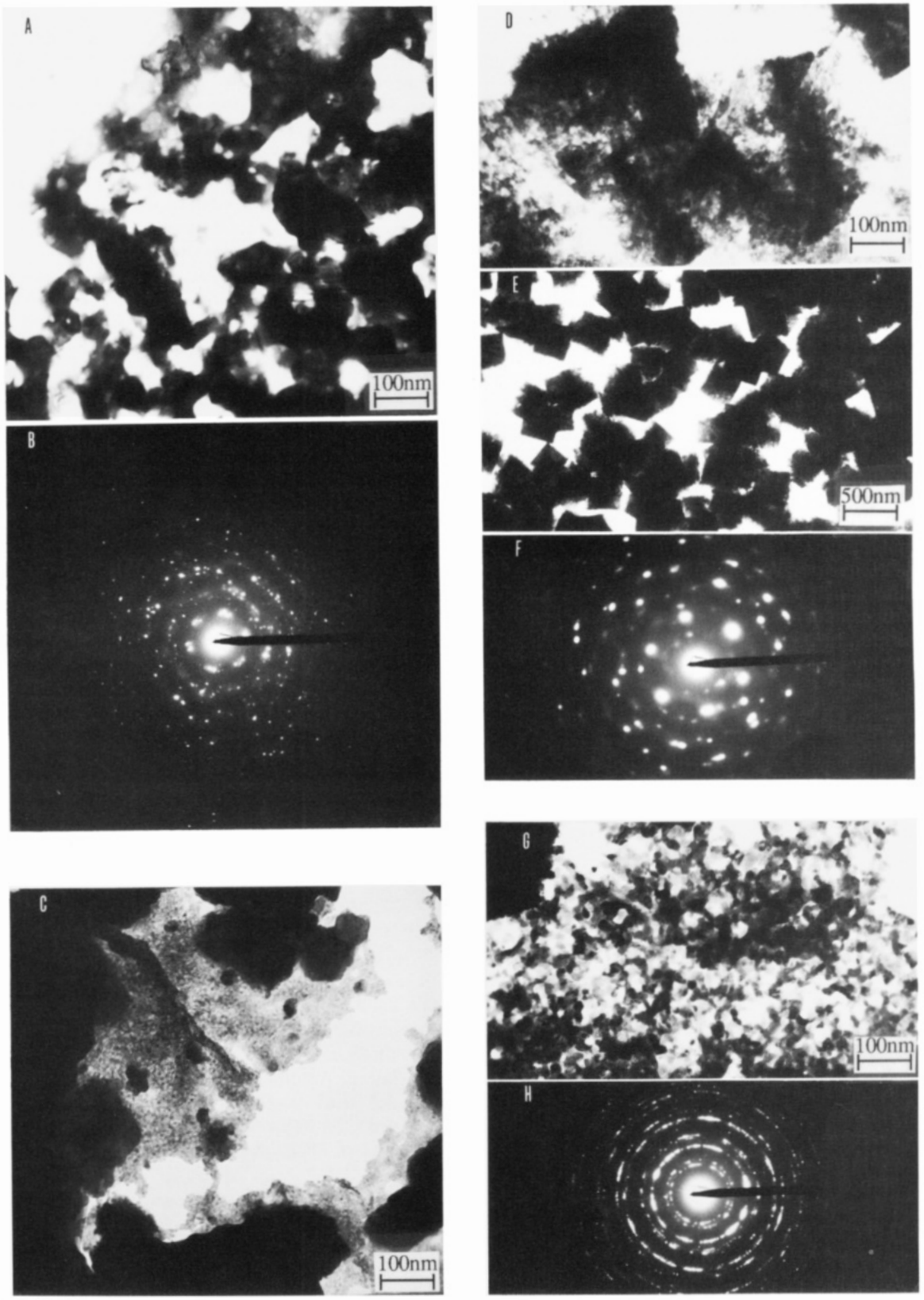

Figure 16. TEM image (A) and ED (B) of Pb–OH–C before reaction with Na_2SeSO_3; TEM image after 3 min reaction (C); TEM (D, E) and ED (F) after 6 min reaction; (G) and (H) as (D, E) and (F) but a different region of the specimen.

in Figure 1c. It should be stressed that this pH increase occurs in a selenium-free solution. In a selenosulfate-containing solution, an even greater pH increase occurs, and an explanation for this increase (for both CdSe and PbSe deposition) has been suggested based on the decomposition of the selenosulfate.[9] For the equivalent selenium-free Cd solution, no increase in pH was observed, which indicates a difference in the chemistry of the two solutions.

The nucleation experiments on Au substrates (Figure 2) show that Pb–OH, which is quite adherent (it is not rinsed off by water), deposits on the substrate within a few minutes of immersion of the substrate in the Se-free solution (in the Se-containing solution, only PbSe

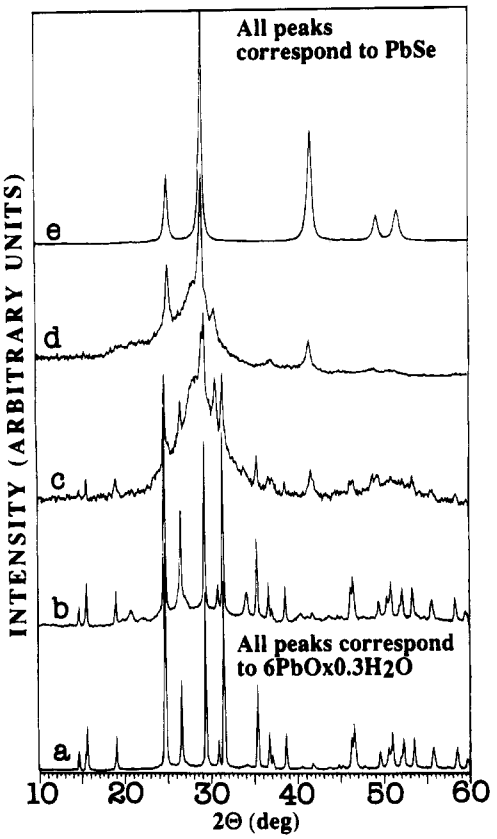

Figure 17. XRD spectra following the process of PbSe formation from the reaction of $PbO{\cdot}0.3H_2O$ (Pb–OH) and Na_2SeSO_3. Pb–OH before reaction (a); after 1.5 min reaction (b); after 3 min (c); after 4.5 min (d); after 6 min (e).

is observed). This is similar to the nucleation behavior of CdSe [7] with the one difference that in Se-containing solutions, it appears that $Cd(OH)_2$ forms first on the substrate and is slowly selenized to CdSe while the corresponding selenization of Pb–OH is considerably faster, and only fully selenized PbSe is seen in the early stages of deposition.

The TEM data in Figure 4 show, in agreement with the results for CdSe and the previous XRD data for PbSe,[9] smaller crystallites from the LC bath than from the HC bath. However, these data show additional, important information on the films. While the HC films are made up of only large crystallites (the terms "large" and "small" are used in the relative sense here), the LC films contain domains of mainly small crystallites but also some large ones. In addition, the large-crystallite domains in the LC films only occur after a certain thickness (>ca. 30 nm) is attained. The XRD spectrum of the *LC* deposits in Figure 7a is dominated by the large crystallite domains. The apparent presence of broad peaks, on which the sharper peaks ride, allows only an approximate estimation of crystallite size from these spectra. However, as shown in Table 2, there is good agreement between these estimations and the TEM results. The crystallite sizes estimated for the HC films are also in reasonable agreement with the TEM results.

It appears from the above results that either the smaller crystallites are transformed into larger ones at certain sites on the substrate or nucleation of the larger crystallites occurs at voids which are seen to occur in the very thin films.. This could either be a substrate effect (variations in nucleation) or local concentration changes at certain regions. Since we showed that large crystallites could be formed even in the presence of solid hydroxide for PbSe, it is clear that there is a delicate balance between the two mechanisms and thus formation of the two crystallite sizes in the LC films. As the deposition proceeds, Pb ions will be removed from the solution due to formation of PbSe. The TSC concentration, however, should remain constant. Thus the TSC:Pb ratio will decrease, resulting in a decrease in the concentration of solid hydroxide–a trend which will favor the ion-by-ion mechanism. This trend will be offset to a greater or lesser extent by the gradual increase in pH as the reaction proceeds. The cross-sectional TEM results (Figure 5) showing the homogeneity of the crystallite size throughout the film thickness argues against such an effect. Also, experiments with multiple depositions of very thin films, each time from a fresh solution, indicate that while there is somewhat less formation of larger crystallites in this case compared with the same thickness deposited from a single solution, the large crystallites still develop. Therefore these results support a mechanism whereby small crystallites continue to form on previously deposited crystallites, while large crystallites nucleate at sites on the substrate where such adsorption did not occur and continue to grow in the form of large crystallites. The ion-by-ion mechanism by which these larger crystallites grow is slower than the cluster growth (since a higher selenide concentration is required in the former case), and we see this also experimentally. Thus, for very thin films, the ion-by-ion growth has not had time to begin (too low a selenide concentration), and only small crystallites, formed by the cluster mechanism, are observed. We do not know why certain regions of the substrate are more or less favorable to either Pb–hydroxide cluster adsorption and/or to ion-by-ion deposition; it may be that there are regions of different surface properties (physical or chemical heterogeneity) on the substrates.

The LC depositions show the apparent presence of a matrix surrounding the individual PbSe crystallites. The TEM/ED and HRTEM study of this matrix (Figure 6) indicates that it is amorphous and possesses a very similar characteristic length parameter to the crystalline lattice parameter. The TEM/EDS microanalyses indicate that there is no difference in composition between the matrix and the crystals and that the matrix is therefore (at least predominantly) PbSe.

The results of the chemical analyses comparing LC films with matrix and HC films essentially without matrix were not entirely conclusive. While it is clear that there is some excess of Pb relative to Se, particularly for the LC films, there is no evidence that this is due to the matrix. The XPS results (Table 3) show that the surface of the individual crystallites are oxygen rich (as would be expected). Also, the smaller (LC) crystallites are more oxygen rich and Se deficient than the larger (HC) ones, which could be explained by the higher surface-to-volume ratio of the former. It is possible that oxygen not only adsorbs on the surface (both as a Se–oxide for the LC as-deposited films as well as other chemisorbed or physisorbed states) but also partially substitutes for the Se.

Biró et al.[14] studied the effect of annealing temperature on the electrical resistivity of CD PbSe. They found a sudden drop in the resistivity of their films upon gradual heating and suggested an explanation whereby the as-deposited film consisted of small crystals of PbSe surrounded by an amorphous matrix of PbSe. They also noted that their results could be explained by the presence of elemental Se between the PbSe crystallites, which had been previously reported in evaporated PbSe films.[15] Differential thermal analyses supported the presence of elemental Se in their results. Our results show direct imaging of this amorphous matrix and support assignment of its composition as PbSe. The lower than stoichiometric Se:Pb ratios found by us, particularly at the early stages of deposition where the matrix is mainly found, argue against any appreciable amount of elemental Se occurring in the films.

Since the PbSe films from the TSC bath are formed, to a greater or lesser degree, via an intermediate Pb–OH species, separation of formation of the latter from its selenization reaction gives some clues to the overall mechanism of deposition. Since Pb–OH–C forms films while we could obtain Pb–OH only as a precipitate (although in principle, films of this composition could probably be obtained using the chemical deposition technique with, e.g., urea as a slowly generated hydroxide source), we investigated the former first. The selenization proceeds by breaking down relatively large crystals of Pb–OH–C to very small crystals of PbSe and also amorphous material (Figures 15 and 16). Large cubic PbSe crystals, covered with much smaller crystals, eventually form. It is clear, as well as interesting, that the final PbSe film is different from one normally deposited insofar as the latter does not form the large cubic crystals. This gives us another method to deposit these films with different properties. However, the formation of the small crystals and in particular, formation of the matrix, occurs in the selenization reaction independent of whether the selenization occurs along with (or, more accurately, after a short time of) formation of the Pb–OH–C or after a film of Pb–OH–C is independently formed. The formation of the large cubic crystals only from predeposited Pb–OH–C may be connected with the high local concentration of the Pb precursor in this case. The equivalent selenization reaction of the Pb–OH precipitate proceeds in a similar manner (Figure 17).

The growth and, particularly evident for Pb–OH, the decrease in the intensity of the broad amorphous peak (Figures 15 and 17) suggest that the PbSe crystallites grow from the matrix. Samples such as that in Figure 6A suggest likewise, as it would be difficult to explain why such a large amount of matrix surrounds individual crystallites if crystal growth *preceded* matrix formation.

NTA–Complex System. A fundamental difference between the TSC and NTA complexes of Pb is that the latter, being a stronger complexant, can give solutions where no solid phase is present. In this respect, the Pb/NTA system is similar to the Cd/NTA system in that a sharp boundary exists between the LC and HC depositions. Since Pb is known to form only a single 1:1 complex with NTA, the solution will be either turbid (NTA:Pb < 1) or free of any solid phase (NTA:Pb > 1), with only a very narrow range (when NTA:Pb is close to unity) where a solid phase occurs in a visibly clear solution. In this respect, it differs from CdSe deposition, where two different complexes exist and the 1:1 complex is relatively weak, allowing a wide range of compositions where a solid phase occurs in a visibly clear solution.

As might be expected, there is no fundamental difference between the LC films from the TSC and NTA baths; in both cases a solid phase is present at the start of the deposition. The HC films do differ, however. The difference is not so much in the size of the individual crystallites in the films (there is a factor of 2 difference—see Table 2), but rather in the manner by which these crystallites aggregate in the film. In the TSC films, the crystals aggregate into approximately spherical clumps of ca. 200 nm size, with relatively large voids between the clumps (Figure 3B). This explains the light scattering and nonreflecting matte appearance of these films. The clumps and voids are of the same order of size as the wavelength of light, compared with the relatively even distribution of crystals (which themselves are too small to scatter light) in the aggregates themselves. As the films become thicker, the voids will gradually fill up, explaining the improved transmission of these films as they become thicker. In the NTA films, the crystals are distributed fairly homogeneously throughout the films and the individual crystallites appear to be better connected (Figure 8B and 9D). Thinner films scatter light because of the voids in these nonhomogeneous films. While we offer no specific reason for the difference between the two types of HC films, it is likely that it can be ascribed to the fact that, in contrast to the HC TSC bath, the corresponding NTA bath is completely free of an initial solid phase and only the ion-by-ion mechanism can occur.

Hydroxide–Complex System. The low-temperature LC films of all thicknesses deposited from this system are made up solely of very small crystals (Figure 11A), very similar to the LC films from TSC complex with low selenosulfate concentrations, but lacking the domains of large crystals which the thicker TSC films exhibit. The reason for this difference is not obvious. While the deposition rate of the HC films is somewhat slower than that from the other two complexes (when it might be argued that the relative rates of ion-by-ion and cluster reactions would favor the latter), the same is true—even more so—for the LC films which have a very slow rate of deposition. It may be that the concentrated hydroxide-containing solutions perform an efficient in situ substrate cleaning function.

The low temperature HC films—made up of large (micron sized) cubes together with aggregates of small crystallites—are very different from the other HC films but similar to the films formed by selenization of Pb–OH–C layers. This difference could be explained by the high pH of these solutions (ca. 14 compared with ca. 13.4 of the LC solutions). We showed previously that high-pH solutions (pH ca. 14) cause an increase in crystal size of nanocrystalline CdSe films[16] and find this also

(14) Biró, L. P.; Darabont, Al.; Fitori, P. *Europhys. Lett.* **1987**, *4*, 691.

(15) Gobrecht, H.; Niemeck, F.; Boeters, K. E. *Z. Phys.* **1960**, *159*, 533.

(16) Hodes, G.; Howell, I. D. J.; Peter, L. M. In *Photochemical and Photoelectrochemical Conversion and Storage of Solar Energy*; Tian, Z. W., Cao, Y. Eds.; International Academic Publishers: Beijing, China 1993; p 331.

to occur for PbSe films. The mixture of small and large crystallites obtained in the 0 °C HC films suggests that the conditions are close to the transition between small and large crystallite deposition. This pH effect is the subject of a separate study and is only mentioned here as a possible phenomenological explanation for the large crystal size in these films at high pH (large free hydroxide concentration). While the mechanism seems connected with enhanced mobility of surface atoms, probably through dissolution and reprecipitation, we do not have enough evidence at this stage to support this, or any other mechanism. Temperature also plays an important role in this pH effect due to the strong decrease in the ion product of water with increase in temperature as well as kinetic enhancement of the crystal growth. Thus at higher temperatures, the same concentration of hydroxide translates into a lower value of pH. The LC films deposited at 60 °C can therefore be affected at a lower pH than those deposited at 0 °C giving larger crystals (Figure 11d). The increase in crystal size resulting from higher temperatures in the HC films can be likewise rationalized.

The hexagonal crystals obtained for HC deposition at 80 °C (Figure 13) appear to represent a new phase of PbSe (composition confirmed by microprobe analysis) although we cannot rule out the possibility of a $PbSeO_x$ compound, since microprobe analysis does not detect oxygen. The XRD spectrum (Figure 14) does not correspond to any known compound of this type. Computer simulation of this spectrum is theoretically consistent with a rhombohedral form of PbSe. A more detailed investigation of this material will be carried out.

Acknowledgment. We thank Ivan Kuzmenko for advice and assistance with the computer simulation of the hexagonally shaped PbSe and Yuval Golan for help and advice with electron microscopy and for the gold substrates. A.A-Y. thanks Dr. A. K. Petford-Long for help with high resolution work during her sabbatical at the Department of Materials, University of Oxford.

CM950049H